



Optimisation applied to composite marine propeller noise

N. Lex MULCAHY¹; Paul CROAKER²; Damian G. McGUCKIN³;

Paul A. BRANDNER⁴; Nicole KESSISSOGLOU⁵

^{1,2} School of Mechanical and Manufacturing Engineering, UNSW Australia & Pacific ESI, Australia

³ Pacific ESI, Australia

⁴ University of Tasmania (AMC), Australia

⁵ School of Mechanical and Manufacturing Engineering, UNSW Australia

ABSTRACT

In the design of maritime vessels, the reduction of noise and vibration is of primary importance for the comfort and safety of passengers and crew, the reliable operation of sensitive instruments on research vessels and the acoustic signature of military vessels. One of the main sources of noise and vibration is the propeller. Shape-adaptive structures, which adapt their shape to changes in their operating conditions, have a number of applications including marine propellers. Previous studies of shape-adaptive propellers have concentrated on maximising the efficiency of the propeller, either in a ship's disturbed wake flow or at off-design conditions. In the present work, a method is developed to determine whether propellers with flexible composite blades can be designed to radiate less underwater noise than equivalent rigid propellers. An optimisation procedure, which adjusts the composite material properties in order to minimise the radiated sound, is applied. The core of the procedure is the radiated sound computation, which processes the results of a transient hydroelastic analysis to compute the sound power on a porous surface that surrounds and translates with the propeller. The results of a computation for a flexible propeller are compared to those of a rigid counterpart.

Keywords: Composite, Propeller, Optimisation I-INCE Classification of Subjects Number(s): 13.5, 54.3

1. INTRODUCTION

The main sources of noise on a ship are machinery, propulsors (for example, propellers), pumps and fans (1). For propellers, much of the noise will be transmitted into the water. At low power, noise can come from the hydrodynamic forces produced by the propeller operating in a non-uniform wake, while at higher powers, much greater noise levels can be produced if cavitation occurs. Noise that is internal to the ship is a concern as it can affect the crew's performance and passengers' comfort. For military vessels, the noise transmitted into the water provides a signal on which hostile weapons can home, thereby compromising the stealth of the vessel. The same noise can also interfere with a warship's own sensors and hence reduce sensor effectiveness (1).

Shape-adaptive structures have properties that allow them to adapt to their working conditions through geometrical changes and can be found in a number of applications, for example, yacht booms, marine propellers, floor panels and pump impellers (2). A shape-adaptive propeller is flexible and designed so that the blades deform with load changes in such a way that the propeller performance is enhanced in comparison to that of a conventional "rigid" metal propeller. Shape-adaptability can be achieved through the choice of the appropriate blade geometry and the optimum arrangement of composite materials. Its goals may include higher efficiency over a greater range of operating conditions, or reduced cavitation and noise.

¹ lexm@esi.com.au

² p.croaker@unsw.edu.au

³ damianm@esi.com.au

⁴ p.brandner@utas.edu.au

⁵ n.kessissoglou@unsw.edu.au

The present work has developed a method to minimise the radiated sound from a flexible composite marine propeller. The methodology is outlined in section 2, a numerical example is presented in section 3 and concluding remarks are given in section 4.

2. ANALYSIS

2.1 Scenario and Optimisation

The scenario considered is one of a ship travelling at constant speed with propulsion by a single propeller. In this scenario, the thrust provided by the propeller must equal the resistance to longitudinal motion. When a ship without a propeller is towed, the water pressure distribution on the hull produces a certain resistance, while the same ship with an operating propeller has a different hull pressure distribution and generally increased resistance. Often this second case is treated as a deduction in effective propeller thrust due to the change in pressure on the hull so its equilibrium equation is

$$R = T(1 - t) \quad (1)$$

where R is the towed resistance, T is the propeller thrust and t is the thrust deduction factor (3).

The composite layup of the propeller and possibly the pitch as well, are adjusted to minimise the radiated sound power at a number of observer stations travelling with the same direction and speed as the ship.

In the present analysis, the resistance R is considered to be only a function of ship speed V_s , the thrust T is primarily a function of propeller rotation rate n , usually in revolutions per second, and all other factors are held constant. The thrust deduction factor t is also assumed constant. In this work, thrust is the average thrust over one cycle of rotation of the propeller. Ship speed is specified, and therefore resistance is fixed, so that Equation 1 can be solved for the propeller rotation rate to produce the required thrust. A root-finding method (4) can be used for this purpose but is only convenient when the thrust can be computed quickly, such as for a rigid propeller with axisymmetric inflow. However, for the case of a flexible propeller and spatially non-uniform inflow, the root finding method is not suitable. For this latter case, the propeller rotation rate is treated as an optimisation variable and the thrust-resistance equality is imposed as a constraint equation.

2.1.1 Objective Function

The general optimisation problem is the minimisation of the objective function f by adjusting the design variables x_i and at the same time satisfying some constraints g_j . In the present analysis the objective function is the radiated sound power W computed on a sphere enclosing the propeller

$$f = W. \quad (2)$$

The centre of the sphere is located at the origin of the coordinate axes, which is also the centre of the propeller. The Sequential Least Squares Programming optimisation algorithm (SLSQP) is used (5, 6). Gradients of the objective function with respect to the design variables are required by the SLSQP algorithm and are estimated using a forward finite difference expression given by

$$\frac{\partial f}{\partial x_i} \approx \frac{f(x_i + \varepsilon) - f(x_i)}{\varepsilon} \quad (3)$$

where ε is a small number. Typically, ε is taken to be a proportion of the difference between the specified upper and lower bounds of variable x_i .

2.1.2 Design Variables

The propeller blades are constructed of anisotropic composite layups for which the coupling between the bending and twisting actions results in what is called bend-twist behaviour (7). The composite layup for a blade section consists of many plies, with each ply being a combination of fibre and matrix materials. Changing the composite layup alters the amount that the propeller blades twist under load and consequently the amount the propeller pitch changes with load. Orthogonal ply properties are associated with the in-plane longitudinal and transverse directions. The angle the longitudinal direction makes to a reference direction is called the ply angle. The plies are grouped into sets with four different ply angles in the present work. One set has a ply angle θ_1 and the other sets are relative to this angle, namely θ_1+45° , θ_1-45° and θ_1+90° (Figure 1). The proportion of plies at angle θ_1 is designated p_1 , with the remainder of plies evenly divided between the other ply angles. It is assumed that there are a large number of plies of equal thickness and the plies at any angle are uniformly distributed throughout the thickness. The section elastic properties may then be calculated using a

smearred approach with a mixture rule (7).

The available design variables are (a) the change in ply angle $\Delta\theta_1$, (b) the proportion of plies in the main direction p_1 , (c) the change of the propeller pitch to diameter ratio $\Delta P/D$, and (d) the propeller rotation rate n . Only some of these design variables may be active in any given analysis.

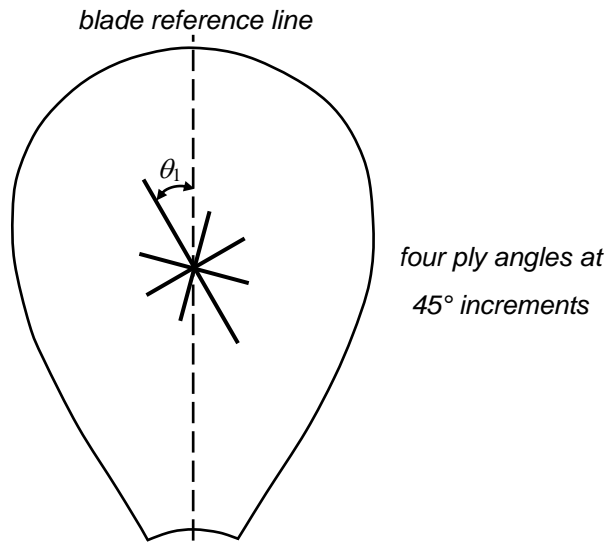


Figure 1 – Ply angle definition

2.1.3 Constraints

In addition to the specified upper and lower bounds of the design variables, either one or two constraint equations may be imposed:

- a) The thrust-resistance equation given by Equation 1 is imposed as an equality constraint

$$g_{eq} = \frac{T(1-t)}{R} - 1 = 0 \quad (4)$$

- b) Optionally, in-plane surface strains may be limited by the inequality constraint

$$g_{ieq} = 1 - \max\left(\frac{\varepsilon_i}{\varepsilon_{i(\text{limit})}}\right) > 0 \quad (5)$$

where ε_i denotes normal strains ε_{11} , ε_{22} or shear strain γ_{12} computed at the top and bottom surfaces for the each of the possible ply directions, and $\varepsilon_{i(\text{limit})}$ being the corresponding specified limiting values of the strains. Therefore, all surface strains are constrained to be within limiting values. The tensile and compressive limits for the normal strains, ε_{11} and ε_{22} , may be different.

Gradients of the constraint equations are required by the SLSQP algorithm and are computed in a similar manner to the gradients of the objective function.

2.2 Hydroelastic Analysis

Computation of the fluid-structure interaction of the flexible propeller and the water is necessary as the fluid velocities and pressures depend on the geometry of the deformed blade, while the structural deformations and blade geometry depend on the fluid pressures. This hydroelastic analysis is achieved by combining a hydrodynamic panel code and a structural finite element code. The hydrodynamic code is a modification of the panel code by Brandner (8), which in turn is an extensive modification of the NASA Ames PMARC code (9). Parts of the structural analysis code are based on PCFEAP, a small general purpose finite element analysis program (10,11).

In the hydrodynamic analysis, the coordinate axes translate and rotate with the propeller, so that the solution can be found for a flow problem in which the propeller is at rest in a moving fluid. The flow field around the propeller is assumed to be inviscid, irrotational and incompressible. For this case, if the velocity vector \mathbf{V} is related to the total velocity potential Φ by

$$\mathbf{V} = -\nabla\Phi \quad (6)$$

the velocity potentials satisfy Laplace's equation

$$\nabla^2 \Phi = 0. \quad (7)$$

Fluid velocity fields \mathbf{V} are assumed to be composed of two parts – the onset flow velocity \mathbf{V}_{in} , which includes the effect of frame rotation, and the perturbation velocity \mathbf{V}_p . Similarly, the total velocity potential Φ is composed of the onset flow potential φ_∞ and the perturbation velocity potential φ .

The propeller surface is modelled by a mesh of constant strength source and doublet panels. The wake sheet, assumed to be of zero thickness, has constant strength doublet panels only. Following the formulation of Ashby et al. (9) the governing equations of the hydrodynamic analysis are

$$\mathbf{A}\boldsymbol{\mu} + \mathbf{W}\boldsymbol{\mu}_w + \mathbf{B}\boldsymbol{\sigma} = \mathbf{0} \quad (8)$$

where \mathbf{A} , \mathbf{W} and \mathbf{B} are arrays of coefficients, $\boldsymbol{\mu}$ is the vector of doublets on the structure surface, $\boldsymbol{\mu}_w$ is the vector of doublets on the wake, and $\boldsymbol{\sigma}$ is the vector of sources on the structure surface. There is one equation per surface panel. In terms of potentials, the surface doublet μ and source σ values are respectively given by

$$\mu = \frac{\varphi}{4\pi} \quad (9)$$

$$\sigma = -\mathbf{n} \cdot \frac{(\nabla\Phi - \nabla\varphi_\infty)}{4\pi} = \frac{(\mathbf{n} \cdot \mathbf{V}_s - \mathbf{n} \cdot \mathbf{V}_{in})}{4\pi} \quad (10)$$

where \mathbf{n} is the outward facing normal vector to the surface and \mathbf{V}_s is the surface velocity vector. Arrays \mathbf{A} and \mathbf{W} are modified so as to impose the Kutta condition at the blade trailing edges. This is achieved by setting the doublet strengths on the first row of wake panels equal to the difference in doublet strengths of the two rows or columns of surface panels whose common edge forms the separation line at the trailing edge. Wake doublets are found from the Kutta condition for the panels adjacent to the trailing edge, and are propagated along the wake with time. Equation 8 can be solved for the surface doublet values of the panels. Once the surface doublets are known, the surface velocities and pressures can be calculated. To calculate the surface velocities, the gradient of the potential is required. Finite differences of the panel doublet strengths have typically been used to calculate these gradients. However for highly distorted panel geometry the gradients predicted using finite differences can have poor accuracy. Here the k -exact reconstruction technique of Barth and Frederickson (12) has been used to calculate the doublet gradients. The k -exact reconstruction technique creates a k^{th} order polynomial of the doublet within each panel through a constrained least squares approximation of the surrounding panel doublet values. Once the polynomial coefficients have been determined, the doublet gradient can readily be determined by differentiating the polynomial. The k -exact reconstruction technique has successfully been applied to flow induced noise problems by Croaker et al. (13).

The most straightforward way of computing the fluid-structure interaction is to transfer the surface pressures to the structural analysis, compute the deformed shape and velocities, and then transfer this information back to the hydrodynamic analysis to begin another iteration. Unfortunately, this loosely coupled process is prone to instability. In the present work, the governing hydrodynamic equations are for a rigid propeller in combination with structural equations that have been modified for an added mass effect of the water to account for the contribution of structural motion to the fluid pressures:

$$\mathbf{A}\boldsymbol{\mu}_r + \mathbf{W}\boldsymbol{\mu}_w + \mathbf{B}\boldsymbol{\sigma}_r = \mathbf{0} \quad (11)$$

$$(\mathbf{M} + \mathbf{M}_h)\ddot{\mathbf{u}} + (\mathbf{C} + \mathbf{C}_h)\dot{\mathbf{u}} + \mathbf{K}\mathbf{u} = \mathbf{P}_r \quad (12)$$

where \mathbf{M} is the mass matrix, \mathbf{M}_h is the hydrodynamic added mass matrix, \mathbf{C} is the damping matrix, \mathbf{C}_h is the hydrodynamic damping matrix, \mathbf{K} is the stiffness matrix, \mathbf{P}_r is the vector of hydrodynamic loads acting on the rigid structure, \mathbf{u} is the structure nodal displacement vector and the dot superscripts denote differentiation with respect to time. Terms in Equation 11 are similar to Equation 8 but for rigid components and with $\mathbf{V}_s = \mathbf{0}$ in Equation 10. The equations are solved iteratively: given $\boldsymbol{\mu}_w$ and $\boldsymbol{\sigma}_r$ the hydrodynamic equations for the current configuration are solved for $\boldsymbol{\mu}_r$; the surface fluid pressures are calculated and fed to the structural computation to give the structure loads \mathbf{P}_r ; the structural equations are solved for nodal displacements \mathbf{u} and velocities $\dot{\mathbf{u}}$; and then the deformed shape of the propeller and surface normal velocities are returned to the hydrodynamic computation. After convergence of the structure displacements, the fluid velocities and pressures are calculated from a solution of the hydrodynamic equations including surface motion given by Equation 8.

Modal superposition using Williams' mode acceleration method (14,15) and the SS22 time-stepping algorithm (11) are used to solve the structural equations. The structure is modelled by

quadrilateral elements constructed by superimposing four triangular shell elements. The triangular shells are based on a shear deformable plate bending triangle (16) and an optimised membrane triangle with drilling freedoms (17). Blades are assumed to be fixed at their connections to the hub.

2.3 Acoustic Analysis

The radiated sound power calculations are based on the solution of the convective Ffowcs Williams-Hawkings (FW-H) equations for moving sources in a uniformly moving medium by Najafi-Yazdi et al. (18). The FW-H equations (19) are based on the equations of mass and momentum conservation of a fluid which is partitioned by a mathematical surface into interior and exterior regions. The motion of the fluid on and exterior to the surface corresponds to that of the real fluid, while that of the interior is specified arbitrarily. Mass and momentum sources maintain the flow discontinuity at the surface and these sources act as sound generators. The governing equations are then conservation equations with sources which are valid throughout the fluid, although only the exterior region is of interest. The convective FW-H solution is an extension of Farassat's Formulation 1 and 1A (20), and is called Formulation 1C. It is applicable to both impermeable and porous surfaces. In the present analysis the propeller surfaces are impermeable. Scattering of noise by the ship is not considered, nor the presence of the water surface, volume noise sources or diffraction around the propeller edges. It should be noted that the panel code does not resolve any flow turbulence and hence the predicted far-field sound will consist entirely of tonal noise at harmonics of the blade passing frequency. At these frequencies the wavelength of the sound is far greater than the propeller diameter, chord and trailing edge thickness and hence diffraction around the propeller edges will be negligible.

The present implementation uses the advanced time approach in which the source or emission time is the main variable and the arrival time at the observer is calculated. Acoustic pressure histories at observer points are calculated based on the pressure and velocity histories of the propeller surface panels. The observer points are distributed on a sphere surrounding the propeller. The propeller is treated as if it is rotating, but otherwise stationary, in a mean flow equal to the ship speed but with opposite direction. The surface panel pressure and velocity histories are for a common sequence of times which correspond to the time step sequence of the hydroelastic analysis. In general, while emission times for the noise radiated from all panels are the same, arrival times at the observer points are all different. The travel time depends on the distance between the surface panel and an observer point at the emission time along with the Mach number of the mean flow, which is small. At a given observer, the pressure history due to one surface panel will be for a particular sequence of arrival times, while the pressure history due to another panel will be for another time sequence. To enable the accumulation of observer pressures due to all surface panels, the various pressure histories are interpolated at common observer times. Similarly, observer normal velocity histories are calculated with normal velocity as follows

$$v_n = \frac{p \cos \theta_{nR}}{\rho V_s} \quad (13)$$

where p is the acoustic pressure, θ_{nR} is the angle between the radiation vector $\tilde{\mathbf{R}}$ (source to observer) (18) and the normal vector \mathbf{n} at the observer, ρ is the water density (1025 kg/m^3) and V_s the speed of sound in water (1500 m/s).

Each observer has an associated tributary area on the surface of the sphere. The pressure and normal velocity histories are used to compute the radiated sound power on the sphere as follows

$$W = \frac{1}{\Delta t} \int_A \int_0^{\Delta t} p v_n dt dA \quad (14)$$

with the integration performed over the sphere surface area A and averaged over the time interval Δt , the latter being approximately equal to the period of rotation.

3. NUMERICAL EXAMPLE

3.1 Description

To ascertain whether optimisation of the flexible composite propeller material properties may be beneficial in reducing sound radiated into the water, a simplified situation has been considered with propeller 4381 from Boswell (21) operating at near its design condition in a four-cycle wake (22). Propeller 4381 has five blades and zero skew and zero rake, as shown in Figure 2. Boswell and Miller

(22) measured the inflow velocity field for a four-cycle wake in water tunnel tests. The wake was created by a wake screen within the circular cross-section of the water tunnel upstream of the measurement point. The circular section was divided into eight equal sectors by wire meshes. The effect of the wake screen was to produce higher than average velocities on alternate sectors and lower than average velocities on the others. A plot of the ratio of the axial velocity V_x to the average velocity V is also presented in Figure 2.

The propeller with diameter D of 5.0 m, rotation rate n of 2.0 revolutions per second and average inflow velocity V of 8.9 m/s had an estimated thrust T of 530 kN. Thrust deduction was zero, so the required resistance R was set as 530 kN. The ship speed V_s is equal to the average inflow velocity V .

Structural material properties for a carbon-epoxy composite with 40% volume fraction were estimated from the data in Soden et al. (23) and are presented in Table 1. Ply angle 1 (θ_1) can vary in the range from -90 to +90 degrees with the angle measured from the midline of the blade, and the proportion of plies (p_1) at θ_1 can vary between 0.25 and 0.7. For this example, the surface strains were not constrained.

The radiated sound power for the carbon-epoxy composite propeller was computed on a sphere of radius 15 m, with 3600 observer points. For comparison, the radiated sound power was also computed for three other cases corresponding to a rigid propeller in open water conditions, a rigid propeller in the four-cycle wake, and a metal propeller (nickel-aluminium-bronze) in the four-cycle wake. Material properties for the metal propeller, based on data from Carlton (3), are also presented in Table 1.

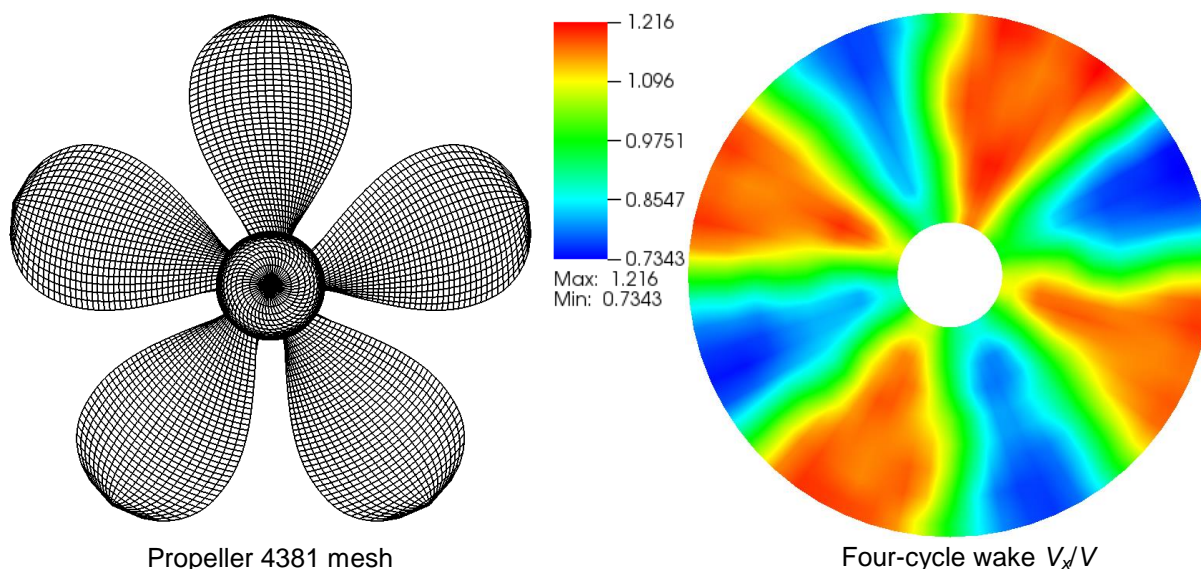


Figure 2 – Propeller 4381 mesh and four-cycle wake velocity field

Table 1 – Propeller material properties

	Composite	Metal
Elastic modulus 1 (GPa)	93.9	122
Elastic modulus 2 (GPa)	7.1	122
Poisson’s ratio	0.28	0.34
Shear moduli (GPa)	3.1	45.5
Density (kg/m ³)	1500	7600

3.2 Results and Discussion

A summary of the results of the four cases analysed is presented in Table 2. The composite propeller results are for ply angle 1 (θ_1) equal to 8.7 degrees and the proportion of plies (p_1) at θ_1 equal to 0.66 (which is near the specified upper limit of 0.7).

Table 2 – Summary of results

	Rigid propeller (open water)	Rigid propeller (4-cycle wake)	Metal propeller (4-cycle wake)	Composite propeller (4-cycle wake)
Rotation rate (rps)	2.0438	2.0435	2.0370	2.0362
Efficiency	0.6271	0.6260	0.6263	0.6267
Sound power (W)	0.000004	1.035	2.081	1.566

Radiated sound power for the rigid propeller in open water conditions is small compared to the other cases which have disturbed inflow from the 4-cycle wake. For a rigid propeller in open water conditions, only the thickness noise term of the FWH equations contributes to the far-field sound and it has recently been demonstrated that the thickness noise of a marine propeller is negligible in the far-field (24). For the cases with disturbed inflow the rigid propeller has the lowest radiated sound, the metal propeller has the highest and the optimised composite propeller is intermediate between the other two. The shape-adaptivity of the optimised composite propeller is not sufficient to compensate for the deleterious effect of the disturbed inflow. This suggests that it may be better to try to reduce the noise resulting from the disturbed inflow through geometrical changes to the propeller (for example, skew) (25) prior to incorporating optimised composite materials. Nevertheless, the results indicate that for a given propeller geometry the radiated sound power can be significantly reduced by using an optimised composite layup instead of metal. For the case considered here the optimized composite propeller achieved a reduction of approximately 25% in the radiated sound power over the metal propeller, without affecting the hydrodynamic efficiency of the propeller.

4. SUMMARY AND CONCLUSIONS

A method for optimising the composite laminate of a flexible marine propeller so as to minimise the sound radiated into the water has been outlined. A gradient method, that repeatedly runs a hydroelastic analysis followed by an acoustic computation, is used to seek the minimum. Results for propeller 4381, a five-bladed zero skew propeller, operating in a four-cycle wake inflow, show that both a nickel-aluminium-bronze metal propeller and an optimised carbon-epoxy composite propeller produce more noise than a rigid propeller in the same disturbed flow conditions. The optimised composite propeller is better than the metal propeller but the improvement due to shape-adaptivity of the composite propeller is insufficient to reduce the noise to below that of the rigid propeller. The results shown here suggest it may be better to minimise the radiated noise through geometrical changes to the propeller prior to incorporating an optimised composite laminate.

ACKNOWLEDGEMENTS

Financial assistance for this work was provided as part of an ARC Linkage Project LP100200687 jointly funded by the Australian Research Council and Pacific ESI Pty Ltd.

REFERENCES

1. Tupper E. Introduction to Naval Architecture. 3rd ed. UK: Butterworth-Heinemann Elsevier; 1996.
2. Kamoulakos A. "INtelligent COMposite PROducts", Final Report submitted to the European Community (Project BE-98-5505, Contract BRPR-CT98-9006); 2002.
3. Carlton J. Marine Propellers and Propulsion. 2nd ed. UK: Butterworth-Heinemann Elsevier; 2007.
4. Brent RP. Algorithms for Minimization Without Derivatives. Englewood Cliffs, NJ: Prentice-Hall; 1973. Ch. 3-4.
5. Kraft. D. TOMP - FORTRAN Modules for Optimal Control Calculations, Fortschritt-Berichte VDI Reihe 8 Nr. 254, VDI-Verlag, Dusseldorf; 1991.
6. Kraft D. Algorithm 733: TOMP - Fortran modules for optimal control calculations, ACM Transactions on Mathematical Software (TOMS), Association for Computing Machinery, 1994;20(3):262-281.
7. Mulcahy NL, Prusty G, Gardiner CP. Optimisation of composite adaptive response with experimental validation, In: Topping BHV and Papadrakakis M, editors, Proceedings of the Ninth International Conference on Computational Structures Technology, Civil-Comp Press, Stirlingshire, United Kingdom,

- 2008, paper 6.
8. Brandner P. Steady Panel Method Analysis of DTMB 4119 Propeller, in 22nd ITTC Propulsion Committee Propeller RANS/Panel Method Workshop Proceedings, 5-6 April 1998, Grenoble, France, Gindroz B, Hoshino T, Pykkänen JV, eds.
 9. Ashby DL, Dudley MR, Iguchi SK, Browne L and Katz J. Potential Flow Theory and Operation Guide for the Panel Code PMARC, NASA TM-102851, Jan. 1991.
 10. PC/FEAP A Personal Computer Finite Element Analysis Program, Sept. 1999; <http://www.ce.berkeley.edu/~rlt/pcfeap/>.
 11. Zienkiewicz OC, Taylor RL. The Finite Element Method, 4th ed. Vols. 1 and 2, McGraw-Hill, London; 1987 and 1991.
 12. Barth TJ, Frederickson PO. Higher order solution of the euler equations on unstructured grids using quadratic reconstruction. In AIAA Paper 90-0013, 28th Aerospace Sciences Meeting, 8-11 January 1990, Nevada, USA, 1990.
 13. Croaker P, Kessissoglou N, Marburg S. Strongly singular and hypersingular integrals for aeroacoustic incident fields. International Journal for Numerical Methods in Fluids (under review).
 14. Williams D. Displacements of a linear elastic system under a given transient load. Aeronaut Quart. 1949;1:123-136.
 15. Mulcahy NL. Bridge response with tractor-trailer vehicle loading. Earthquake Eng Struct Dyn. 1983;11:649-665.
 16. Mulcahy NL, McGuckin DG. The addition of transverse shear flexibility to triangular thin plate elements. Finite Elements in Analysis & Design 2012;52:23-30.
 17. Felippa CA. A study of optimal membrane triangles with drilling freedoms. Comput Methods Appl Mech Eng. 2003;192:2125-2168.
 18. Najafi-Yazdi A, Brès GA, Mongeau L. An acoustic analogy formulation for moving sources in uniformly moving media. Proc R Soc A. 2011;467:144-165.
 19. Ffowcs Williams JE, Hawkings DL. Sound generation by turbulence and surfaces in arbitrary motion. Phil. Trans. R. Soc. Lond. A. 1969;264(1151):321-342.
 20. Farassat F. Derivation of Formulations 1 and 1A of Farassat. NASA TM-2007-214853, March 2007.
 21. Boswell R. Design, cavitation performance and open-water performance of a series of research skewed propellers. Technical Report 3339, DTNSRDC, March 1971.
 22. Boswell RJ, Miller ML. Unsteady propeller loading – measurement, correlation with theory, and parametric study. NSRDC Report 2625, October 1968.
 23. Soden PD, Hinton MJ, Kaddour AS. Lamina properties, lay-up configurations and loading conditions for a range of fibre reinforced composite laminates. Compo. Sci. Technol. 1998;58:1011-1022.
 24. Ianniello S. The underwater noise prediction from marine propellers: an essentially nonlinear problem. Proc ICSV 21; 13-17 July 2014, Beijing, China.
 25. Feizi Chekab MA, Ghadimi P, Reza Djeddi S, Soroushan M. Investigation of different methods of noise reduction for submerged marine propellers and their classification. Am J Mech Eng. 2013;1(2):34-42.